The impact of subglacial drainage system evolution and glacier lake outburst on Arctic fjord macronutrient dynamics: Kongsfjorden, Svalbard

Andreas Alexander[1,2,3,4]; Livia Piermattei[4,5]; Philipp Assmy[6]; Andrea L. Popp[4,7,8]; Nicolas Valiente[8,9]; Guy D. Tallentire[10]; Simon Filhol[4]; Thomas V Schuler[4]; Ugo Nanni[4]; Jack Kohler[6]; Louise S. Schmidt[4]; Léo Decaux[11]; George Cowie[4]; Allison Bailey[6]; Riko Noormets[12]; Pierre-Marie Lefeuvre[6]; Claire S. Earlie[13]; Maarja Kruusmaa[3]; Andy Hodson[12,14]

[1]Department of Earth Sciences, University of Bergen, Bergen, Norway.

[2]Bjerknes Centre for Climate Research, Bergen, Norway.

[3]Centre for Biorobotics, Tallinn University of Technology, Tallinn, Estonia.

[4]Department of Geosciences, University of Oslo, Oslo, Norway

[5]Swiss Federal Institute for Forest, Snow and Landscape Research (WSL), Birmensdorf, 8903, Switzerland

[6]Norwegian Polar Institute, Fram Centre, Tromsø, Norway

[7]Hydrological Research Unit, Swedish Meteorological and Hydrological Institute (SMHI), Norrköping, Sweden

[8]Centre for Biogeochemistry in the Anthropocene, University of Oslo, Oslo, Norway

[9]Department of Science and Agroforestry Technology and Genetics, University of Castilla-La Mancha, Albacete, Spain

[10]Department of Geography and Environment, Loughborough University, Loughborough, UK

[11]Department of Geomorphology, Faculty of Earth Sciences, University of Silesia, Sosnowiec, Poland

[12]Arctic Geology Department, University Centre in Svalbard, Longyearbyen, Svalbard

[13]Jet Propulsion Laboratory, California Institute of Technology, Pasadena, CA, US

[14]Department of Environmental Sciences, Western Norway University of Applied Sciences, Sogndal, Norway

Corresponding author: Andreas Alexander (andreas.alexander@uib.no)

Key Points:

- We investigate the impact of a glacier lake outburst flood on fjord nutrient delivery
- Nutrient supply is dependent on glacier drainage configuration
- We propose ongoing denitrification in the glacier bed

Abstract

Global warming is amplified in the Arctic, where it leads to increased glacier melt and freshwater runoff, especially from tidewater glaciers. Here, runoff usually enters the fjord at depth; due to its buoyancy, it induces a circulation system that enhances the exchange of energy and matter between the glacier and the marine environment. This has great significance for macronutrient delivery to fjords and thus primary production. However, most studies of these linkages have temporal resolutions well below the expected variability and so the effects of low-frequency, high-amplitude events on the marine environment remain poorly known. In this study, we combine glacier observations with high-frequency fjord and glacier lake sampling to describe the impact of the 2021 glacier lake outburst flood (GLOF) from lake Setevatnet into Kongsfjorden (Svalbard). In doing so, we demonstrate the importance of changing subglacial conditions both before and during the GLOF, and examine their effects upon macronutrient availability in the inner fjord via direct glacial runoff and the buoyancy-driven entrainment of fjord bottom waters. Our observations reveal that direct nutrient subsidy from the glacier is most important in the early summer, providing critical nitrate (NO_3^-) and orthosilicic acid ($Si(OH)_4$) following the routing of meltwater through an inefficient drainage system along the glacier bed. Increasing quantities of ice melt later in the season force the establishment of an efficient drainage system, creating a plume in the inner fjord, and resulting in the onset of a buoyancy-driven circulation, entraining nutrient-rich bottom water. When the sudden drainage of a glacier lake with high NO_3^- concentrations occurred; however, it left little imprint on the NO_3^- content of the inner fjord, and instead induced seasonal maximum nitrite (NO_2^-) concentrations. This surprising outcome implies that NO_3^- was removed by denitrification at the glacier bed and its product NO_2^- was discharged by the flood waters into the inner fjord. Our findings show that the delivery of key, productivity-limiting nutrients (in this case NO_3^- and Si) from tidewater glaciers not only depends on runoff volume, but also on characteristics of the glacier drainage system (inefficient vs efficient), the evolution of which is fueled by high-magnitude events, such as outburst floods.

Plain Language Summary

The catastrophic and rapid drainage of glacier lakes can have huge impacts on surrounding environments. Here, we investigate the effects of the drainage of glacier lake Setevatnet (Svalbard) into the adjacent fjord Kongsfjorden. We show that the lake, despite high nitrate concentrations, fails to deliver this producitivty limiting nutrient to the fjord. Instead, we observe increased concentrations of nitrite, which indicate denitricifaction reactions. This might imply the release of the greenhouse gas nitrous oxide from tidewater glaciers.

1 Introduction

The Arctic is undergoing rapid warming due to anthropogenic climate change (e.g., IPCC SROCC, 2019; Rantanen et al., 2022, Isaksen et al., 2022). The Svalbard archipelago is an epicenter of this change, warming at rates 2-2.5 times more than the Arctic average and 5-7 times more than the global average (Isaksen et al., 2022). As a result, many glaciers in Svalbard have been retreating and thinning since the beginning of the 20th century (Kohler et al., 2007; Schuler et al, 2020; Geyman et al., 2022), with some tidewater glaciers already having retreated onto land (Blaszczyk et al., 2009, Kavan et al., 2023). With increasing rates of glacier melting, greater volumes of freshwater and glacial sediments are released into fjords (van Pelt et al., 2019), altering physicochemical properties (Halbach et al., 2019; Pavlov et al., 2019), fjord circulation

(Torsvik et al., 2019) and contributing to coastal water darkening in Svalbard fjords (Konik et al., 2021). At the same time, more meltwater and rain are stored in ice-dammed lakes, increasing the likelihood of sudden drainage events (e.g. Shugar et al., 2020).

Tidewater glaciers are important foraging areas for seabirds and marine mammals since the discharge of buoyant subglacial water induces a circulation that brings zooplankton to the surface, making them easy prey for surface-feeding predators (Stott, 1936; Lydersen et al., 2014; Bertrand et al., 2021, Hop et al. 2023). The same mechanism can also influence fjord biogeochemistry and primary production through the entrainment of nutrient-rich bottom waters (e.g., Lydersen et al., 2014; Meire et al., 2017; Halbach et al., 2019; Hopwood et al., 2020). Glacier meltwater can acquire nutrients from melting of snow and ice, bedrock weathering and glacial microbial processes (Hodson et al., 2005) and supply them directly to the fjord. However, during summer, when buoyancy-driven freshwater plumes form at the termini of tidewater glaciers, the entrainment of nutrient-rich deep marine waters likely enhances this nutrient release (Meire et al., 2017; Kanna et al., 2018; Hopwood et al., 2018; Halbach et al., 2019, Cape et al., 2019; Hopwood et al., 2020, Williams et al., 2021). Without this effect, runoff from tidewater glaciers would likely limit primary production through nutrient dilution (if the meltwater inputs are nutrient-poor) or through light limitation by highly turbid water (Halbach et al., 2019).

Each summer, runoff of meltwater along the surface of glaciers leads to the formation of supraglacial streams, which eventually propagate to the glacier bed via moulins and crevasses. There, water flows towards the glacier terminus, either via an inefficient, distributed drainage system, or via an efficient channelised drainage system (Flowers, 2015). As the melt season progresses, the subglacial drainage system evolves from an inefficient system towards a channelised one, often manifested by the formation of large sediment plumes where channels enter the ocean in front of tidewater glaciers (How et al., 2017). Once the melt rate drops towards the end of summer, ice creep closes the channels, thereby shutting off plume circulation and its associated sediment transfer. With reestablishment of an inefficient drainage system, residence times of water at the glacier bed increase, promoting significant rock-water-microbe interactions that influence the macronutrient content of any runoff that eventually leaves the system (Hodson, 2008; Wadham et al, 2010). Other important biogeochemical processes can also occur in association with channelized drainage system development. For example, nitrate (NO_3^-) removal via denitrification seems most likely in the distributed system, causing depletion of this critical, productivity-limiting nutrient (Wynn et al, 2006). In contrast, transfer of surface-derived meltwater, nutrients, oxygen and organic matter can support aerobic processes in sediments that flank the channelized system, resulting in increasing NO_3^- concentrations through nitrification (Hodson et al, 2008; Tranter et al, 2005). However, whilst NO_3^- is a key limiting nutrient in Svalbard fjords (e.g. Halbach et al, 2019), the extent to which glacial nitrification or denitrification can influence NO_3^- availability in fjord ecosystems remains unclear. Similar uncertainty also surrounds the subsidy of lithogenic nutrients, apart from $Si(OH)_4$ (Hopwood et al, 2020; Meire et al, 2017) and iron (Arrigo et al. 2017), which tend not to be limiting in the Arctic.

Most current studies focusing on the impact of tidewater glaciers on fjord biogeochemistry are either based on long-term monitoring at fixed locations, often distal to glacier calving fronts (Juul-Pedersen et al. 2015; Assmy et al. 2023) or are limited to short periods during the melt season (Meire et al. 2017; Halbach et al. 2019). Thus, most studies do not capture ephemeral but

potentially critical glacier discharge events and their impact on fjord hydrology and biogeochemistry (Hopwood et al., 2020). These can, for example, be associated with the establishment of the efficient channelized drainage system, or with sudden drainage of ice-dammed lakes, such as glacial outburst floods (GLOFs). The latter are glacier lakes that suddenly release their stored volume due to dam failure. Reports from indigenous communities have indicated negative impacts of GLOF events on marine life, mainly due to the large volumes of freshwater and sediments stressing resident marine organisms (Kjeldsen et al., 2014; Schiøtt et al. 2022). Kjeldsen et al., (2014) suggested potential benefits of GLOFs to marine ecosystems via enhanced entrainment of bottom water, thereby increasing fjord nutrient levels and primary production. However, there are so far no quantitative studies showing the impact of GLOF events and other high-amplitude low-frequency runoff events on fjord macronutrient levels.

This study investigates the impact of drainage system evolution, culminating in a clearly delineated GLOF event, and the associated macronutrient dynamics, within a well-known fjord ecosystem, Kongsfjorden (Svalbard). We describe the collection of 2.5-months (June – August 2021) of environmental data used to examine the links between glacier dynamics, subglacial hydrology and nutrient dynamics within a fjord ecosystem significantly influenced by tidewater glaciation and annual GLOFs.

2 Materials and Methods

We applied a highly interdisciplinary approach to monitor the effects of the 2021 Setevatnet GLOF event in Kongsfjorden, Svalbard, in close vicinity of the Ny Ålesund Research Station (Figure 1). Ground observations at the lake, the glacier and the fjord were supplemented with water sampling for chemical analysis, conductivity, temperature, depth (CTD) profiling and multibeam bathymetric surveys at the glacier front, and satellite-based observations of fjord and glacier behaviour (an overview of all collected data can be found in Supplementary Figure S0). This study focuses on the observations in the fjord and combines them with observations at the lake and of the glacier.

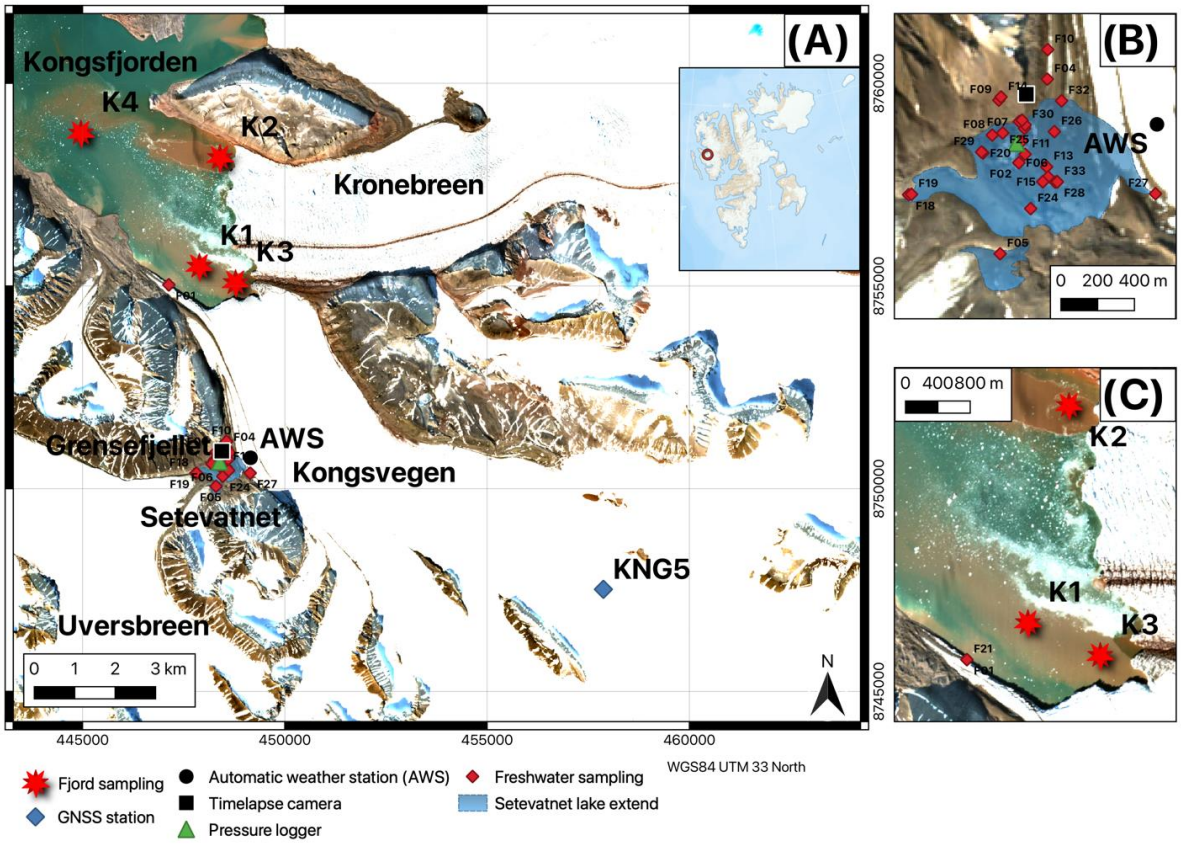

Figure 1. The location of Setevatnet and all sampling and instrument sites. (A) Overview of all sites and the location of the study site on the Svalbard archipelago. (B) Close up view of the Setevatnet site with freshwater sampling locations (F02-F34). (C) Close up view on the sampling sites for seawater (K1-K4) and subglacial sampling (F01&F21) close to the glacier margin. Background image: ESA Sentinel-2, 01 August 2021.

2.1 Field site

The High Arctic Svalbard Archipelago is currently undergoing rapid climatic warming (Isaksen et al., 2022). Kongsfjorden is a 4-10 km wide and over 30 km long fjord on the west coast of the main island, Spitsbergen. Water masses within the fjord are a mix of Arctic and Atlantic water, freshwater from glacier melt and terrestrial runoff, as well as winter-cooled water, formed through surface cooling and convection in autumn and wintertime (Cottier et al., 2005). Several tidewater glaciers terminate in the fjord, among them Kronebreen and Kongsvegen, at the southeastern end of the fjord.

2.2. Glaciology

Kongsvegen (78° 48’N, 12° 59’ E) is a roughly 25-km long north-west oriented glacier with a surface slope ranging from 0.5° to 2.5° (Hagen et al., 1993). Continuous mass balance

monitoring has been conducted since 1987 (NPI, 2023). Kongsvegen is a surge-type glacier in quiescent stage (Melvold&Hagen 1998).

Setevatnet lies 4 km upstream of the glacier front at the south-western margin of Kongsvegen (78° 48.9’ N, 12° 36.8’ E). It is situated in a small valley at the junction of Kongsvegen to the north, the glacier Uvêrsbreen to the south, the mountain Grensefjellet to the west and the mountain Gåvetoppen to the east (Figure 1). Snow and ice melt leads to the formation of the lake, followed by annual GLOF events, as first described by Liestøl (1976). During the drainage event, all of the lake water drains through Kongsvegen and into Kongsfjorden.

Surface velocities of Kongsvegen are recorded as part of the mass balance monitoring program conducted by the Norwegian Polar Institute. A GNSS (Global Navigation Satellite System) instrument mounted on the mass balance stake KNG5 (78.792537 °N, 13.058108°E) records data at 5-second intervals. Data were differentially post-processed to derive hourly static positions, using the Norwegian Mapping Authority permanent network base station as reference. Changes in hourly positions were used to derive ice speed.

A weather station installed near Setevatnet (78.81871 °N and 12.6505 °E), part of the wireless sensor network deployed over the whole Kongsvegen glacier (Filhol et al, 2023), includes sensors for measuring air temperature, air pressure, snow depth, wind speed and direction, collected at 10-minute intervals. The station was installed on 1 May 2021 and collected data until 12 August 2021.

2.3 Hydrology

2.3.1 Hydrological measurements at Setevatnet

A stage-volume relation for Setevatnet was produced using drone-derived orthoimages of the lake when full, and a reference digital elevation model (DEM) generated from Pléiades stereo satellite images from 20 September 2020 when the lake was empty. As the topography of the periglacial area around the ice-dammed lake could be assumed to have remained constant during the winter, the Pléiades DEM provided bathymetry data representative of the lake bottom and elevation with a spatial resolution of 1 m prior to its filling. The drone orthoimage (resolution of 0.2 m) was collected on 21 July 2021, two days before the lake began to drain on 23 July. The drone images were processed in Agisoft Metashape using the standard Structure from Motion workflow (James et al., 2017), which included ground control points (GCPs) for camera orientation. The 18 GCPs show an RMSE of 0.35 m. Only the lake boundaries in stable areas were considered (Figure 2a, blue lines), i.e., where no uplift occurred during the formation of the lake. The water surface line was converted into points with a sample distance of 10 m and their elevation was derived from the Pléiades DEM and averaged to represent the maximum surface elevation (i.e., 195 m as of 21 July). Uncertainty in lake volume originates from the DEM elevation (derived from the Pléiades images), the horizontal accuracy of the drone orthoimage, and the digitization of the lake boundary, with the elevation reading is the main source of error. Assuming an elevation uncertainty of ±1 m (equivalent to the resolution of the DEM), the relative volume uncertainty can be determined from the stage curve.

Water level was recorded using a combination of a pressure transducer and terrestrial time-lapse photography. From the Pléiades DEM we could produce a stage-volume curve (Figure 2d). The onset and early progress of the lake's drainage was determined using a HOBO U20L-02 water level data logger (±0.3% FS raw pressure accuracy). However, since the pressure logger could not be placed at the deepest point of the lake. A stationary tripod-mounted time-lapse camera (Canon EOS 700D, EF50 mm f/1.8 II lens, 30 min interval) was used thereafter. These photographs were used to determine the end of the lake drainage, when no more water was visible in the lake basin.

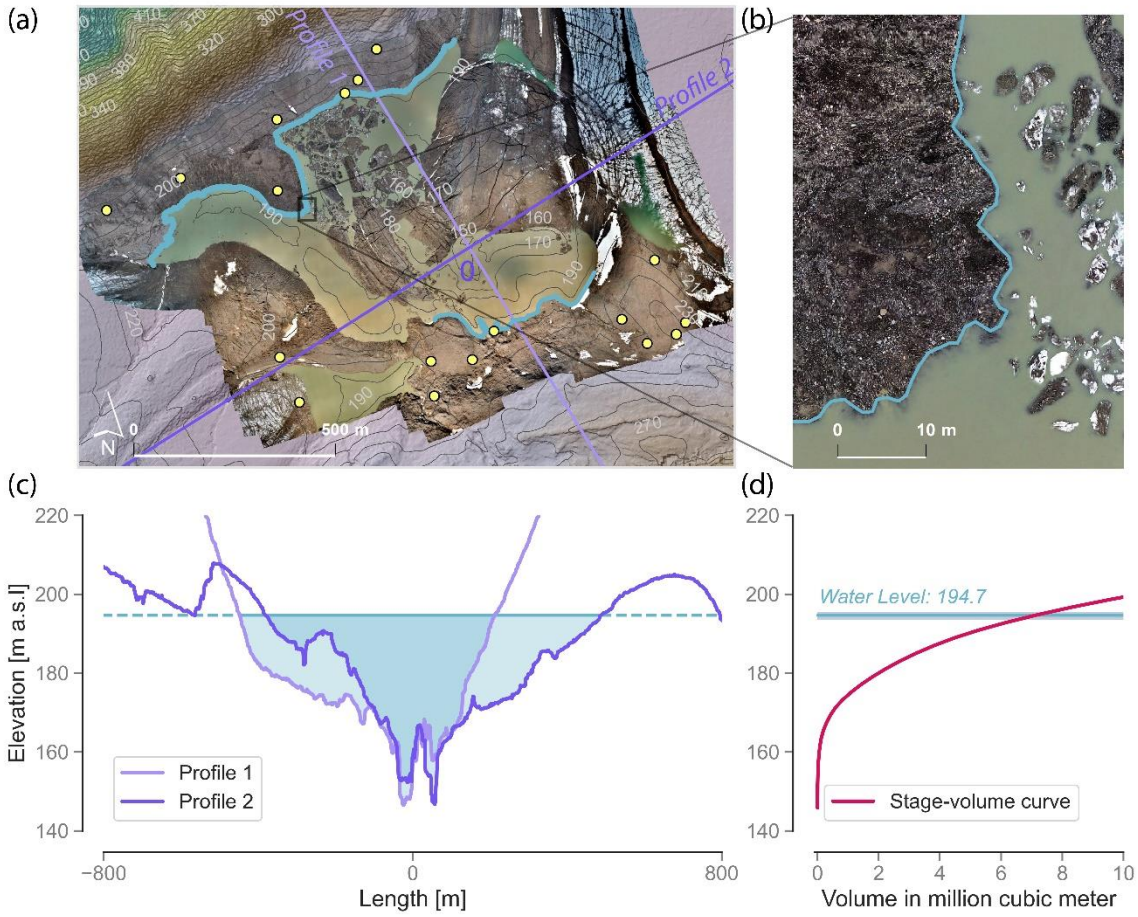

Figure 2: Estimating the volume of the ice-dammed lake from the intersection of the water level observed in the drone orthoimage and the Pléiades DEM. a) Drone orthoimage superimposed on hillshade of the Pléiades DEM, together with corresponding 10-m contour lines. GCPs are indicated by yellow dots. b) Inset showing manual mapping of the water level at a scale of 1:200. c) Two cross-profiles of the Pléiades DEM; profile length is relative to the intersection point of the two profiles. The horizontal line shows maximum elevation of the mapped water level. d) Stage-volume curve derived from the DEM of the reference Pléiades and the water level; uncertainty of the water level elevation varies between ±1 meter.

2.3.2 Meltwater production and runoff

Daily simulations of meltwater production and runoff in the Kongsfjorden region were derived using the CryoGrid Community model (Westermann et al, 2023), an open-source model developed for climate-driven snow simulations in the terrestrial cryosphere. It uses a full energy-balance model and a spectral snow albedo scheme, which follows a slightly altered CROCUS (Vionnet et al, 2012) snow scheme. The specifics of the model are described in detail by Westermann et al. (2023) and Schmidt et al. (2023). In this study, the model is forced by meteorological fields of temperature, humidity, wind, radiation and mass fluxes from AROME-ARCTIC weather forecasts at a 2.5 x 2.5 km horizontal resolution. Given the simple geometry of Kongsvegen glacier, we calculated the runoff by integrating all grid points over the glacier area. Evaluation of the model forcing and output for Svalbard is described in detail in Schmidt et al. (2023).

2.3.3 Fjord Hydrology

During the fieldwork, seawater was regularly sampled at 4 points(Figure 1A): K1 (78.860501°N, 12.583076°E, depth 48.6 m), K2 (78.884674°N, 12.601520°E, depth 44.3 m), K3 (78.857211°N, 12.625304°E, 25.6 m depth) and K4 (78.8888°N, 12.440800°E, depth 98.2 m). Conductivity, temperature and depth (CTD profile) were measured at all 4 seawater sampling points (Figure 1A) using a portable VWR PHenomenal PC5000H meter with a VWR C011 conductivity/temperature probe for all sampling dates except on the 7 August 2021. The resolution was 0.1 mS cm^{-1} for conductivity and 0.1 °C for temperature measurements (accuracy ±1% of the measured conductivity and ±0.2°C for temperature). All conductivity and temperature values were transformed into absolute salinities and conservative temperatures with the Gibbs-SeaWater Oceanographic Toolbox (McDougall & Barker, 2011) in MATLAB R2022b with the geographic reference location of 78.87 °N and 12.3 °E.

2.4. Water sampling and analysis

A total of 34 freshwater and 172 seawater samples were collected between 08 June and 07 August 2021, at different glacial locations and at four fixed fjord locations of variable distance from the glacier fronts (Figure 1A and Table S2&S3).

Freshwater was sampled from surface streams (snow-fed streams running down the surrounding mountain sides and terminating in Setevatnet), supraglacial channels, the Setevatnet lake, and one subglacial outflow site (Figure 1). The latter offered access to subglacial drainage prior to entry into Kongsfjorden during June via an approximately 300 m long channel. Samples were filtered immediately after sampling using 0.2 µm syringe filters and decanted into unused 20 mL Falcon tubes after rinsing them three times with the filtered sample. Snow and ice samples were melted at room temperature in the marine laboratory in Ny-Ålesund and then filtered and decanted with the same procedure as above. All samples were then stored dark at 4°C until the end of the fieldwork. Analyses for NO_3^- and phosphate (PO_4^{3-}) were conducted on a Dionex ICS-1000 Ion Chromatography System at the Department of Geosciences, University of Oslo water chemistry laboratory. The measurements were calibrated for a calibration range between 0 and 20 mg L^{-1}; the limit of detection was thereby below 0.2 ppm for all anions. PO_4^{3-} was consistently below detection limits in the freshwater samples (i.e., 2.1 µmol L^{-1}). Silicate (SiO_2) was determined on the filtered samples using an Auto Analyzer 3 with a detection limit of 0.06 ppm (1.0 µmol L^{-1}) and an accuracy of ±12%.

Fjord samples for NO_3^-, nitrite (NO_2^-), PO_4^{3-}, and orthosilicic acid ($Si(OH)_4$) were collected at 0, 5, 10 and 20 m depth at each sampling station (K1-4). All samples were filtered using a 0.4 µm syringe filter and transferred into unused 20 mL vials after rinsing them three times with the filtered sample water. They were then stored in dark at -18°C. Post-fieldwork analysis was performed using a colorimetric method (Grasshoff et al., 1983; Gundersen et al., 2022) at the Institute of Marine Research, Bergen, Norway. The detection limits were 0.06 µmol L^{-1} for nitrite, 0.5 µmol L^{-1} for nitrate, 0.06 µmol L^{-1} for phosphate and 0.7 µmol L^{-1} for silicate, respectively.

We separated the fjord nutrient dataset in 5 phases based on the glacier, lake and plume observations described in Section 3.1 and the available sampling dates within the period were hydrological changes at Kongsvegen occurred. Phase I includes samples from 10 June to 22 June, Phase II from 24 June to 15 July, Phase III from 16 July to 21 July, Phase IV from 23 July to 26 July (GLOF event) and Phase V for samples collected on 7 August (Table 1).

3 Results

3.1 Dynamics of the subglacial hydrological system, lake drainage and meltwater plume development

Modelled meltwater runoff starts at the end of June with values of ca. $0.5x10^6$ m^3d^{-1}, and peaks around 16 July due to high surface air temperatures (Figure 3a and 3b). Glacier surface velocity is at ca. 0.05 m d^{-1} until early July reaching a maximum on 18 July of ca. 0.35 m d^{-1}, two days after the melt peak (Figure 3c). Afterwards, ice velocity decreases to values of ca. 0.10 m d^{-1}, except for smaller acceleration events possibly associated with the GLOF event (23 July, reaching ca. 0.15 m d^{-1}) and a late season period of enhanced ablation (following 3 August, reaching ca. 0.20 m d^{-1}). The drainage of Lake Setevatnet starts on 23 July at 19:00 and continues for 77 hours until 27 July at 00:00, when the lake completely drained (Figure 3b). The lake volume reached ca. 7.17 million m^3 ±1.07 million m^3 for an average discharge of 26 ±3.86 m^3 s^{-1}.

On 24 June and 28 June, Sentinel-2 imagery shows the first indication of sediment release from Kongsvegen in the form of a dispersed plume (Supplementary Figure S1a and Table S1). Afterwards, no visible plume is detected from the satellite imagery until 13-14 July when a minor sediment release from Kongsvegen is seen (the images were partially cloud impacted and therefore not part of the mapping in Figure S1). On 16 July, we observed a well defined meltwater plume at Kongsvegen via drone survey (Figure S1b). On 17 July, the Sentinel-2 imagery also confirmed a major meltwater plume in front of Kongsvegen, with the greatest areal extent being reached on 22 July. The satellite image from 25 July shows that plumes in front of both Kronebreen and Kongsvegen decreased to about a third of their size (despite ongoing lake drainage from the GLOF), before expanding again on 29 July and then continuing to increase until August (Table S1).

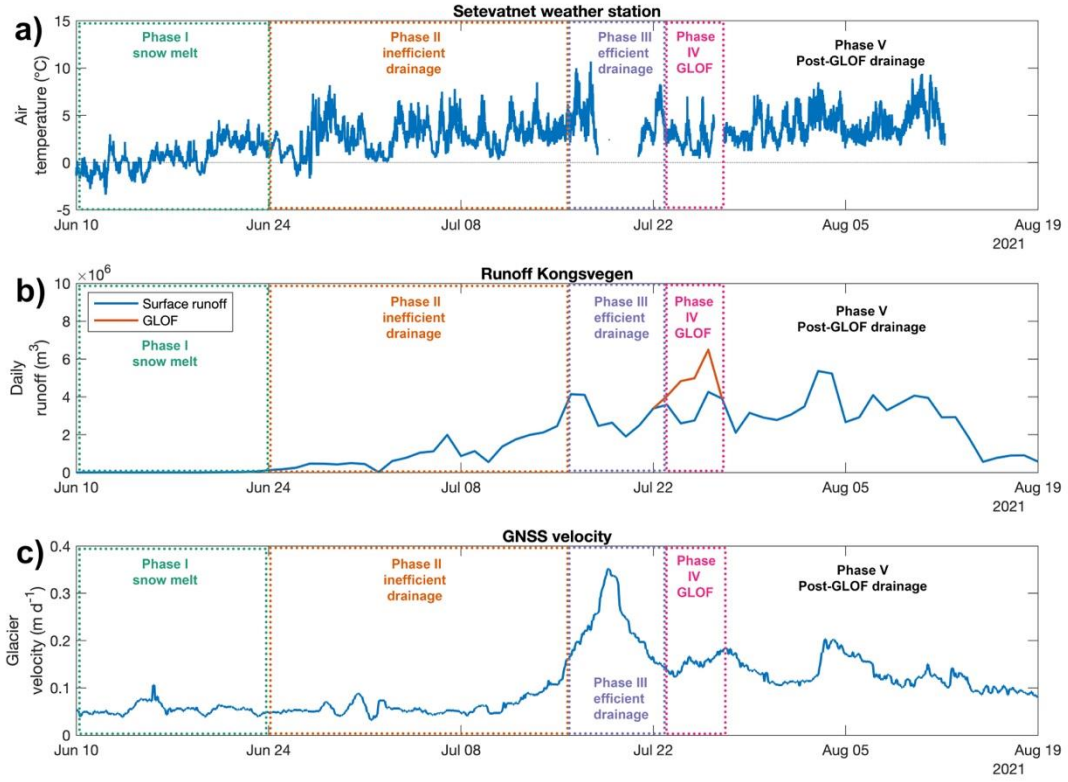

306
307 **Figure 3:** Glacier data A) Air temperature from the automatic weather station located close to
308 Setevatnet (Filhol et al., 2023), B) Simulated surface runoff for Kongsvegen with known lake
309 drainage volume and timing C) GNSS speed at KNG5.
310

311 ### 3.2 Water chemistry

312 The highest nitrate concentration is found in the subglacial water (8.9 µmol L^{-1}, n=1), followed
313 by Setevatnet lake water (mean=5.4 µmol L^{-1}, std=1.3 µmol L^{-1}, [from here on denoted as
314 mean±std] n=20), surface streams (4.2±1.1 µmol L^{-1}, n=4), supraglacial channels (3.8±1.0 µmol
315 L^{-1}, n=4), snow samples (2.3±0.2 µmol L^{-1}, n=3) and ice samples (2.1±0.0 µmol L^{-1}, n=2) (Figure
316 4 and Supplementary Table S2). Nitrate concentrations in the lake show an increasing trend over
317 time (Supplementary Figure 2 and Supplementary Table 2) with the highest concentration of 7.7
318 µmol L^{-1} measured on 17 July, 6 days before the drainage. The lowest nitrate concentration
319 occurred on 20 June with 4.1 µmol L^{-1}. We note, however, that the lake itself was highly
320 dynamic with several isolated side lakes forming, which later merged as the water level kept
321 rising and parts of the glacier around the lake started to uplift.

322

323 Mountain streams running down Grensefjellet exhibit the highest mean silicate concentration
324 (5.5±0.5 µmol L^{-1}, n=4), followed by subglacial water (4.0 µmol L^{-1}, n=1), Setevatnet lake
325 samples (3.2±1.1 µmol L^{-1}, n=20), supraglacial water (1.7±1.5 µmol L^{-1}, n=4). Ice (0.2 ±0.3

326 µmol L^{-1}, n=2), and with the lowest mean concentration in snow samples (0.2 ±0.3 µmol L^{-1},
327 n=3) show(see Figure 4). The silicate concentrations at Setevatnet itself show a decreasing trend
328 over time (Supplementary Figure 2 and Supplementary Table 2) going from the highest
329 concentration of 4.6 µmol L^{-1} on 15 June to 2.3 µmol L^{-1} on 17 July, 6 days before the drainage.

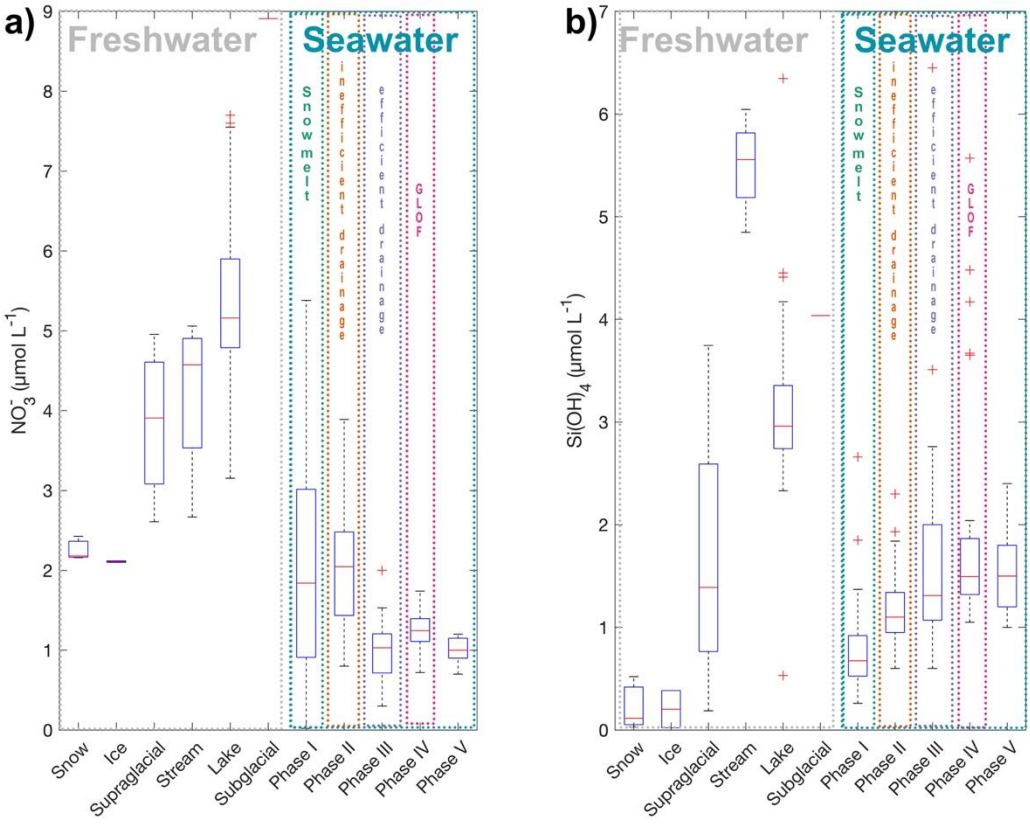

330

331 **Figure 4**. Concentrations of nitrate and silicate in freshwater and seawater samples. Phase I: 10
332 June to 22 June (snow melt). Phase II: 24 June to 15 July (inefficient drainage system). Phase III:
333 16 July to 21 July (efficient drainage system). Phase IV: 23 July to 26 July (GLOF event). Phase
334 V: 7 August (fully developed drainage system).

335

336 3.3 Nutrient variations in the fjord

337 Over the whole fjord area, the three inorganic nitrogen species, NO_3^- and NO_2^-, and PO_4^{3-}
338 showed a general decline, while silicate concentrations showed a gradual increase (Figures 4 and
339 5; Table 1). The decline in NO_3^- and PO_4^{3-} is relatively steep at first (during June), while by mid-
340 July concentrations stabilize at around 1 µmol L^{-1} ±0.4 NO_3^- and 0.2 µmol L^{-1} ±0.0 PO_4^{3-} (Table
341 1). The decline in NO_3^- is more pronounced than for PO_4^{3-}, and maintains NO_X^-: PO_4^{3-} ratios
342 (Supplementary Figure S3e) well below the Redfield ratio of 16:1. Both NO_3^- and PO_4^{3-}
343 concentrations increase slightly during the GLOF event (Table 1). However, there is an increase
344 in the NO_2^- concentrations more pronounced than concentration of NO_3^- and PO_4^{3-}. $Si(OH)_4$

concentrations gradually increase from <1 µmol L^{-1} to around 2 µmol L^{-1} over the observation period with a clear increase in mean concentrations during the GLOF event (Table 1).

Table 1: Mean and standard deviations (Std) of all fjord samples over all depths (0, 5, 10, 20 m). Phase I: 10 June to 22 June (snow melt). Phase II: 24 June to 15 July (inefficient drainage system). Phase III: 16 July to 21 July (efficient drainage system). Phase IV: 23 July to 26 July (GLOF event). Phase V: 7 August (fully developed drainage system). n notes the number of samples for each phase. All units in µmol L^{-1}.

Phase	Mean NO_3^-	Std NO_3^-	Mean NO_2^-	Std NO_2^-	Mean PO_4^{3-}	Std PO_4^{3-}	Mean $Si(OH)_4$	Std $Si(OH)_4$	n
I (10- 22 June)	2.1	1.5	0.1	0.0	0.2	0.1	0.8	0.4	40
II (24 June- 15 July)	2.0	0.7	0.1	0.0	0.2	0.1	1.2	0.4	56
III (16 -21 July)	1.0	0.4	0.1	0.0	0.2	0.0	1.6	1.1	38
IV (23 -26 July)	1.2	0.2	0.2	0.1	0.2	0.0	2.0	1.3	24
V (7 Aug)	1.0	0.2	0.1	0.0	0.2	0.0	1.5	0.4	16

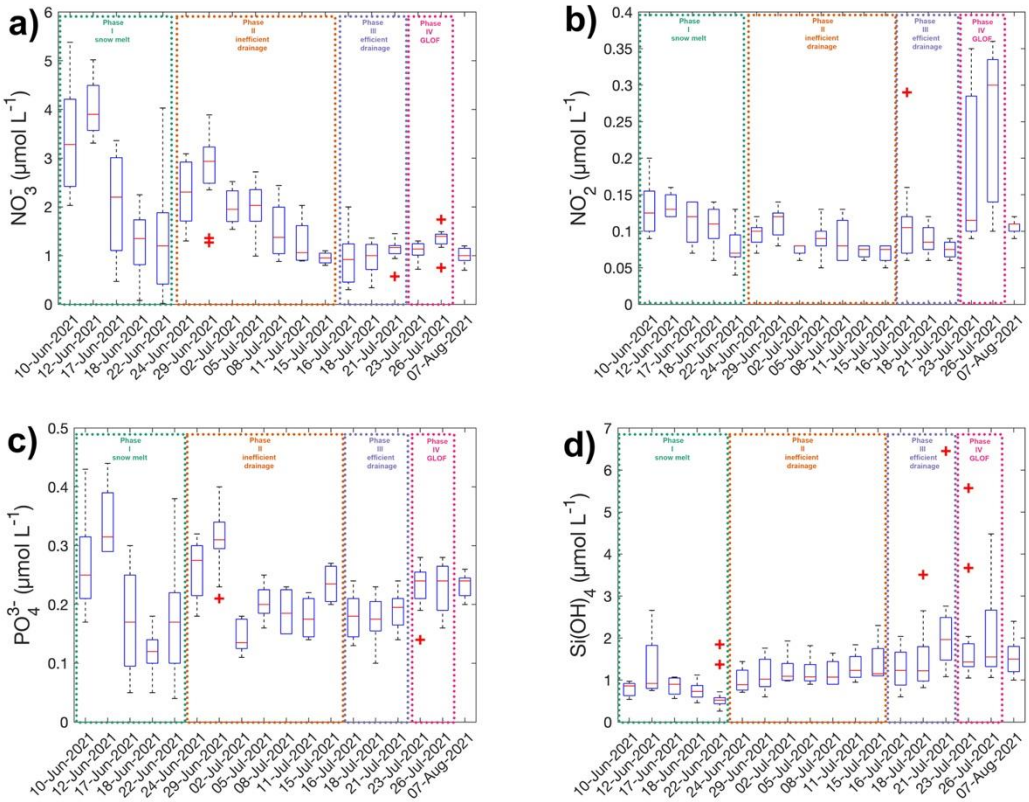

Figure 5: Boxplots showing the temporal evolution of macronutrient concentrations of all sampling stations measured in the fjord.

Before the GLOF event, we observe a positive relationship between NO_3^- and salinity during phase II, and a negative relationship during the other phases (Figure 6). This trend, however, only becomes significant (on a 90% confidence level) during the GLOF event in Phase IV. During Phase I, we observe a slightly negative relationship between NO_2^- and salinity, followed by a slightly positive relationships during the following phases (none of them significant) before the relationship becomes negative again and significant on a 90% confidence level. PO_4^{3-} shows a negative relationship with salinity (not significant), followed by positive trends during the following phases. During the GLOF, this positive trend becomes significant at the 95% confidence level. By far the most significant relationship with salinity exists with $Si(OH)_4$. As time progresses, the correlation between Si concentrations and salinity moves from weak (Phase I) to strong (II and III) to very strong (IV). Therefore, the most significant impact of the GLOF upon the relationships between absolute salinity and nutrient concentration was the consolidation of negative relationships between salinity and NO_3^-, NO_2^- and $Si(OH)_4$ concentrations as well as a positive relationship between salinity and PO_4^{3-} concentrations.

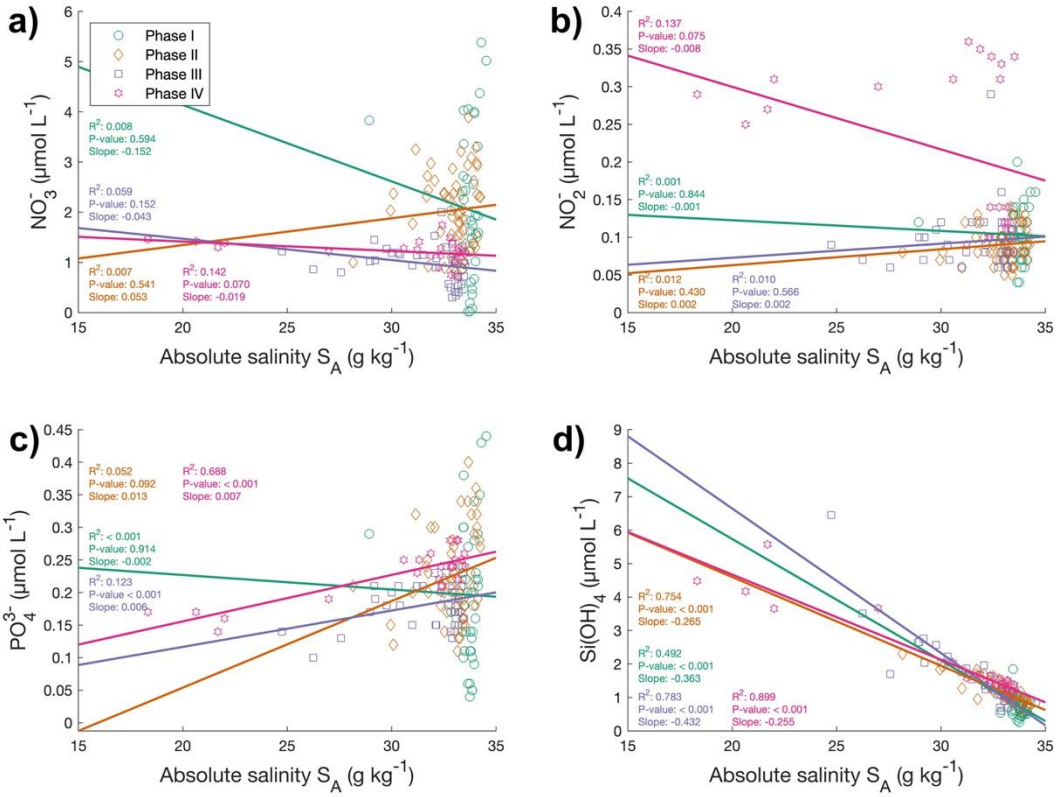

Figure 6: Macronutrient concentrations plotted against absolute salinity throughout the observation period. Phase I: 10 June to 22 June (snow melt). Phase II: 24 June to 15 July (inefficient drainage system). Phase III: 16 July to 21 July (efficient drainage system). Phase IV: 23 July to 26 July (GLOF event). No salinity data were available for 7 August, data after the GLOF event are therefore not part of this figure.

4 Discussion

The observations before, during and after the GLOF event of 2021 provide a unique basis for the description of the impact of glacial drainage system behaviour upon the biogeochemical dynamics of the inner fjord at Kongsvegen. Figure 5 clearly suggests that special emphasis needs to be given to: i) pre-GLOF dynamics, wherein a marked depletion in NO_3^- and PO_4^{3-} was apparent whilst the drainage system was becoming established; and ii) the GLOF itself, when a striking increase in NO_2^- occurred that defies a simple explanation on account of its difference with NO_3^- behaviour. Based on glacier and plume observations, we have subsequenced the dataset in five stages (phase I-V) to explain the different dynamics observed in the fjord. A schematic drawing of occurring processes can also be found in figure 7.

4.1. Pre-outburst flood nutrient biogeochemistry

4.1.1 Phase I (June 10 to June 23)

Supplementary Figure S3 shows that the spring bloom of phytoplankton in Kongsfjorden peaked during mid-May 2021, reducing nitrate concentrations to below 1 µmol L^{-1} and silicate concentrations to the detection limit or lower. Complete silicate utilization therefore points to diatom dominance in the spring bloom. Although the spring bloom was only recorded at a mid-fjord station ~15 km downfjord from the glacier front, phytoplankton uptake during the late bloom period is very likely to have contributed considerably to the initial decline in NO_3^- and PO_4^{3-} at the glacier front stations shown in Figure 5 (see also Supplementary Figures S3). This coincided with the onset of snowmelt in lower elevations in the early half of June, leading to terrestrial runoff from the shoreside into the fjord near the glacier margin. In this period, high concentrations of NO_3^-, NO_2^- and PO_4^{3-} were detectable in both runoff and fjord waters at the immediate glacier margin, suggesting that snowpack nutrient release supplemented the available nutrient resource in the fjord. Snowpack NO_3^- and PO_4^{3-} release has been documented in several studies of the Kongsfjorden glaciers during June, and typically causes a clear, near-exponential decline in meltwater nutrient concentrations through time due to solute elution from the snowpack (Björkman et al., 2014; Hodson, 2002; Hodson, 2006a; Roberts et al., 2010; Spolaor et al., 2021). Svalbard glacial rivers in Kongsfjorden therefore have NO_3^- concentrations up to an order of magnitude greater than the initial parent snowpack during early summer (see Table 4 in Hodson, 2006b); concentrations in rivers drop markedly through time due to a combination of elution and increasing dilution by glacier ice ablation.

4.1.2 Phase II (24 June to 15 July)

During Phase II nutrient concentrations in the fjord increase again, which coincides with the onset of snowmelt at higher elevations. Delivery of nutrients to the fjord is manifested as a visible outflow of a small, distributed meltwater plume along the entire calving front of the glacier by June 28 (Supplementary Figure S1). Nutrient concentration increase in the fjord can again be explained by snowpack nutrient release followed by solute elution and dilution by glacier ice ablation. These processes of non-linear nutrient release are therefore likely to subsidise rapid biological assimilation in the fjord prior to the establishment of efficient subglacial drainage (Phase III). NO_3^- rich fjord bottom waters can thereby not be uplifted until large enough volumes of dilute meltwater create a strong enough buoyant subglacial plume.

Furthermore, the high sediment loads caused by the plume, leading to light limitation for phytoplankton growth (Halbach et al., 2019), will not be delivered to the inner fjord photic zone until enough meltwater is produced (see also Supplementary Figure S1). Rapid, early summer changes in nutrient biogeochemistry at the calving front of the Kongsvegen and Kronebreen glaciers therefore seem to include a short-lived subsidy and prolongation of the spring bloom. The inefficient, distributed drainage system discharges low volumes of snowmelt whose nutrient content is enriched by snowpack elution.

4.1.3 Phase III (16 to 21 July)

In Phase III, glacier ablation rates continued to increase, leading to an increase in ice velocity at Stake 5 that abruptly decreased just prior to the GLOF. The marked deceleration of ice velocities at Stake 5 commenced on 18 July, and suggests that a further critical stage in the development of the subglacial drainage system occurred, leading to even greater connectivity across the glacier bed and a single, dominant meltwater plume in front of Kongsvegen, which started to form on 16 July (Supplementary Figures S1, temperature and salinity data in Figure S3a,c,d and Table S3). During this period, all nutrient concentrations except those of $Si(OH)_4$ decreased (Figure 5, Supplementary Figures S3). The modest increase in $Si(OH)_4$ can potentially be explained by scavenging from the detrital particles in the large turbid plume that formed. For example, amorphous silica may be readily leached from fine subglacial sediment (Hatton et al., 2019). Subglacial erosion has also been shown to have a marked impact upon the yields of $Si(OH)_4$ and PO_4^{3-} to the Kongsfjorden ecosystem (Hodson et al.; 2005; Hodson et al., 2004). However, a shift in biological production towards dominance by non-siliceous phytoplankton is also likely to alter fjord $Si(OH)_4$ dynamics. Such a change also agrees with previous observations of blooms of flagellate algae in the glacier-influenced inner part of Kongsfjorden during the 2017 melt season (Halbach et al. 2019).

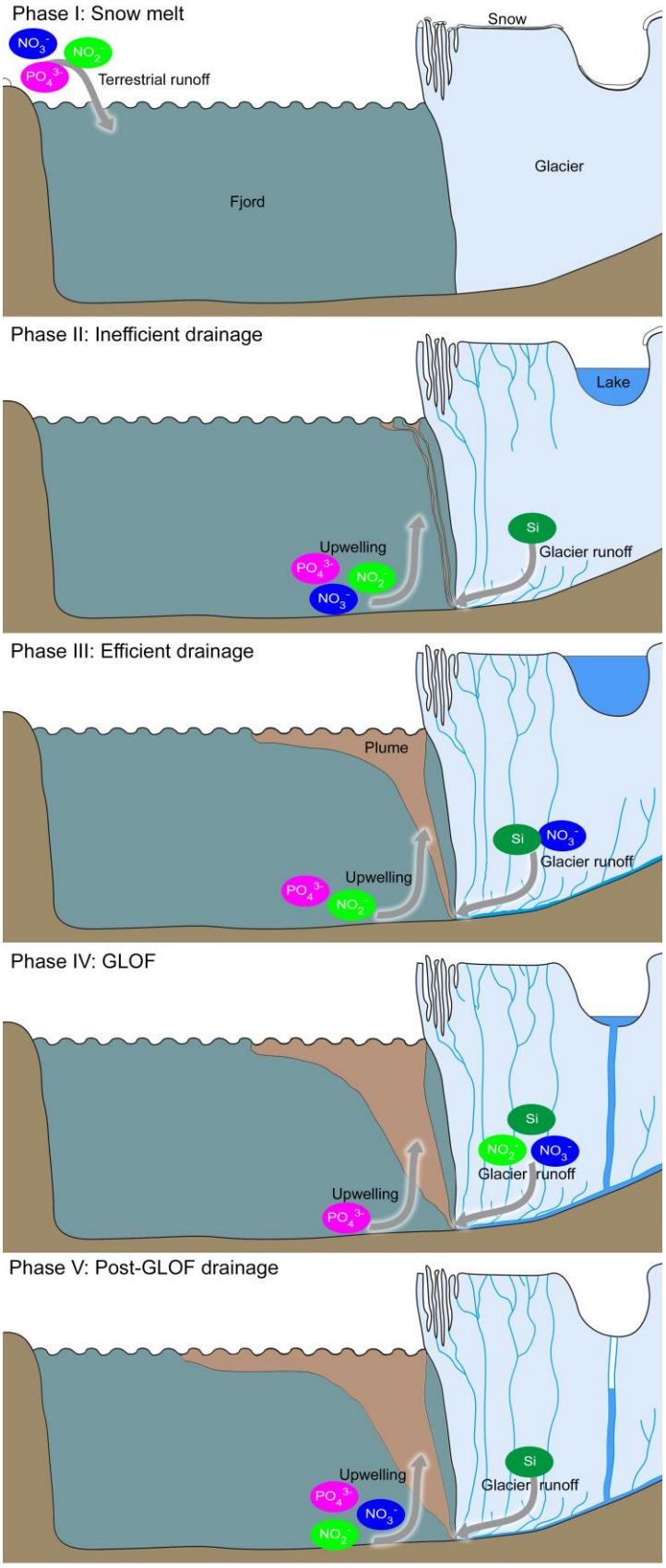
Phase I: Snow melt
Snow
Terrestrial runoff
Glacier
Fjord
Phase II: Inefficient drainage
Lake
Upwelling
Si
Glacier runoff
Phase III: Efficient drainage
Plume
Upwelling
Si
Glacier runoff
Phase IV: GLOF
Si
Glacier runoff
Upwelling
Phase V: Post-GLOF drainage
Upwelling
Si
Glacier runoff

Figure 7: Conceptual overview of glacier hydrological and fjord processes occurring in the inner part of Kongsfjorden during summer and subsequent nutrient release to the marine ecosystem.

4.2. Changes in biogeochemistry during the GLOF (phase IV)

The onset of clear connectivity between the glacier bed and the fjord just prior to the GLOF shows that outburst waters could connect to the existing subglacial drainage system and thus reach the fjord relatively rapidly. However, the low drainage flux (discharge) from the lake suggests that the drainage occurred via a more distributed flowpath than expected based on previous observations by Liestøl (1976). For these reasons, the GLOF (Phase IV, 23 to 26 July) had a positive but limited impact upon nutrients from lithogenic sources (e.g. $Si(OH)_4$), because a large sediment pulse was not observed. Furthermore, no significant effects upon the entrainment of nutrient-rich fjord bottom waters were discernible (Supplementary Figures S3), because the impact of the GLOF upon subglacial discharge was attenuated. However, the increase in NO_2^- was easily discernible (Figure 5), and was unexpected; its origins and consequences warrant further attention.

Nitrite is a highly reactive form of inorganic N that can be formed as an intermediate product during both nitrification and denitrification. Concentrations of NO_3^- and ammonium (NH_4^+) are therefore required to identify the likely mechanism causing the elevated NO_2^- concentrations. However, the utility of NH_4^+ data is often questionable due to its adsorption onto suspended sediment derived from organic matter mineralization, causing its rapid removal in a plume sampling environment. Halbach et al. (2019) have shown high concentrations of NH_4^+ close to the glacier, making nitrification seem plausible within the plume, whilst Wynn et al. (2006) and Ansari et al. (2013) showed nitrification dominates the supply of NO_3^- to glacial runoff from mid-July onwards in Kongsfjorden. However, Figure 5 shows no concomitant increase in nitrification product NO_3^- during the GLOF, suggesting that the mechanism producing the high NO_2^- concentrations might instead be denitrification. Alternative hypotheses, linked to the decoupling of NO_3^- and NO_2^- behaviour during spatially segregated nitrification and NO_3^- assimilation within the fjord plume environment (e.g. Zakem et al., 2018) seem less plausible, because there is no reason why they would be temporally restricted to the GLOF event. The same is the case for nitrification, because high NO_2^- was not observed during other periods of high turbidity within the inner fjord. These changes therefore suggest that the NO_2^- was subglacial in origin, and not associated with the sediment plume in the water.

Although uncommon, denitrification has been detected in the stable isotopic composition of NO_3^- in glacial runoff entering Kongsfjorden (Ansari et al., 2013; Wynn et al., 2006). However, both Wynn et al. (2006) and Roberts et al. (2010) showed that subglacial outbursts from smaller valley glaciers in Kongsfjorden (i.e., Midtre Lovenbreen) initially discharge waters with longer residence times where partial denitrification occurred. These studies, using stable isotopes and mass balance calculations, respectively, also show that outburst waters from the subglacial environment are rapidly replaced by more oxygenated outflows whose content is increasingly enriched by nitrification as summer progresses. Therefore, we hypothesize that the GLOF either displaced waters with long residence times, in which denitrification occurred (perhaps in the deeper subglacial part of the lake itself), or stimulated denitrification through the provision of new NO_3^- and water to anoxic parts of the glacier bed at Kongsvegen. We think the latter mechanism is more likely because we detected an increase in the unstable product NO_2^-. The

gaseous loss of product nitrous oxide (N_2O) means that, in the absence of $d^{15}N\text{-}NO_3^-$ data, NO_2^- is the sole evidence for the event. Consequently, the capacity for the GLOF to fertilize fjord primary production through the provision of productivity-limiting NO_3^- might have, in the case of an incomplete reaction, been offset by the release of N_2O. Indication for a denitrification reaction with release of N_2O is also visible in the results of gas samples taken at Setevatnet in July (Supplementary Table S4). Those samples show a slight oversaturation of N_2O, supporting our hypothesis of an incomplete denitrification reaction with subsequent N_2O release. The GLOF therefore seems to have had little impact upon fjord primary production, either through direct means associated with NO_3^- and $Si(OH)_4$ delivery, or indirect means associated with more vigorous plume upwelling.

5 Conclusions

We investigated the impact of changes in the glacial drainage system of the high-Arctic tidewater glacier Kongsvegen (Svalbard) on the nutrient dynamics of inner Kongsfjorden during summer 2021. We did this from a unique perspective that integrated observations of critical stages in drainage system evolution during the early summer with a novel combination of observations to capture the sudden drainage of the ice-dammed lake Setevatnet. Our work highlights the sensitivity of macronutrient concentrations to drainage system evolution, as the latter influences the direct and indirect supply of productivity-limiting nutrients to an active fjord ecosystem. Direct nutrient supply from glacier meltwater was most important during the late stages of the spring bloom, when high NO_3^- concentrations were likely routed through an inefficient, distributed drainage system. At this stage of the season, the glacial drainage system was principally draining snowmelt whose nutrient concentrations are typically enhanced by snowpack solute elution. However, nutrient supply from fjord bottom waters probably became most important after an efficient, channelised drainage network developed at the glacier bed following 16 July. The establishment of an efficient, channelized drainage system resulted in the visible appearance of a turbid plume close to the glacier front, and therefore marked the beginning of buoyancy-driven circulation that entrails nutrient-rich waters from the fjord bottom and delivers them to the photic zone. Direct nutrient supply from the glacier became markedly less important from this point onwards, with the exception of $Si(OH)_4$.

In late July a GLOF occurred, which we had monitored since early June. We could show that the GLOF had little impact upon nutrient availability in the inner fjord. However, the GLOF was associated with an increase in NO_2^- within the inner fjord, which was likely caused by denitrification in the distributed subglacial drainage system, either via old water displacement or active denitrification during the GLOF event. Contrary to our initial expectations, the GLOF did not enhance the supply of productivity-limiting nutrients (primarily NO_3^- at this stage of the summer) and instead enhanced, denitrification, which likely led to an increased outgassing of the greenhouse gas N_2O. These outcomes demonstrate a complex interplay between tidewater glaciers, their subglacial processes and the marine ecosystem. The role of tidewater glaciers in the supply of nutrients to fjord ecosystems and their effect upon biological production therefore needs to be more carefully investigated with a particular focus on subglacial hydrology and biogeochemistry.

Acknowledgments

We acknowledge scientific input from Jeffrey Andrew Tuhtan, help in the field from Laura Piho, Jaan Rebane and all the folks that occasionally joined us out in the field in June/July 2021. We want to thank the Norwegian Polar Institute and the crew of the Sverdrup station as well as the staff from Kingsbay for hosting us in Ny-Ålesund. The SIOS knowledge center, particularly Inger Jennings for organizational support, UNIS for safety training and logistical support, the master and crew of R/V Clione for their support during the field work in July, Alex Eiler for collection of samples for incubation, Peter Dörsch and Sigrid Trier Kjær at NMBU for the gas analyses. The guests of Mare 10/2021, Birgit Lutz and Cape Race Corporation for help with instrument retrieval in August 2021 as well as Coline Bouchayer and John Hulth for further instrument retrieval.

Funding information

AA acknowledges support from a SIOS Research Infrastructure Access project ('InnovateGLOF') through the Research Council of Norway, project number 291644, Svalbard Integrated Arctic Earth Observing System – Knowledge Centre, operational phase. Further the Robert og Ella Wenzins legat ved Universitetet i Oslo (#292), Familien Stillesen og Professor S. A. Sexes legat (#238), the Hans og Helga Reuschs legat til fremme av studiet av geografi og geologi ved Universitet i Oslo (#208), the Department of Geosciences, University of Oslo, Centre of Biorobotics at Tallinn University of Technology, the Norwegian Research Council Climate Narratives project (grant #324520) and the European Union's Horizon 2020 research and innovation programme under the Marie Skłodowska-Curie grant agreement No 101034309. LP was funded by the Department of Geosciences, University of Oslo and Industrial Liason at the Department of Geosciences, University of Oslo. PA and AB were funded through the Norwegian Polar Institute's Svalbard program and the Research Council of Norway (# 284477). This research is a part of iC3: Centre for ice, Cryosphere, Carbon and Climate and was supported by the Research Council of Norway through its Centres of Excellence funding scheme, project number 332635. NV was funded through the ARCTIC-BIODIVER project (Belmont Forum-BiodivERsA and The Research Council of Norway) and Arctic Field Grant #310631 (The Research Council of Norway). The MAMMAMIA project (NFR grant # 301837) supported the field work and provided data. Simulations of glacier melt rates and associated runoff have been computed for and supported by the Nansen Legacy project (NFR grant # 276730). GDT was supported by a UK Research and Innovation Natural Environment Research Council PhD studentship [NE/L002493/1] and a SIOS Research Infrastructure Access project through the Research Council of Norway, project number 291644, Svalbard Integrated Arctic Earth Observing System – Knowledge Centre, operational phase. ALP acknowledges support through the Arctic Field Grant "GroundPole" granted by the Norwegian Research Council. GC was funded by the Norwegian Research Council Arctic Field Grant (#322678) and the Department of Geosciences, University of Oslo. MK was funded by the EU INTERACT Transnational Access from the European Union's Horizon 2020 project INTERACT, under grant agreement No 730938.

Open Research

All used data can be found in the supplementary information to the manuscript and will be deposited on Zenodo following the peer-review process..

Author contributions

Study design: AA, LP, PA, AH, ALP, NV, TVS, JK, RN
Funding acquisition, fieldwork organization, permits: AA
Field work: AA, LP, LD, GC, MK, RN, AB, GDT
Weather station & data: PML, SF
Glacier velocity: PML
Timelapse camera: JK
Satellite plume analysis: GDT
Setevatnet volume calculation: LP
Runoff simulations: LSS
Incubation experiments: NV
KB3 cholorophyll & macronutrients: PA, AB
Freshwater nutrients: AA, ALP
All other analysis & figures: AA
Manuscript preparation: AA, PA, AH
All authors contributed to the manuscript.

Competing interests:

The authors declare no competing interests.

References

Ansari, A.H., Hodson, A.J., Heaton, T.H.E., Kaiser, J. and Marca-Bell, A., 2013. Stable isotopic evidence for nitrification and denitrification in a High Arctic glacial ecosystem. *Biogeochemistry*, *113*, pp.341-357.

Arrigo, K. R., G. L. van Dijken, R. M. Castelao, H. Luo, Å. K. Rennermalm, M. Tedesco, T. L. Mote, H. Oliver, and P. L. Yager (2017), Melting glaciers stimulate large summer phytoplankton blooms in southwest Greenland waters, Geophys. Res. Lett., 44, 6278–6285, https//doi.org/10.1002/2017GL073583.

Assmy, P., Kvernvik, A. C., Hop, H., Hoppe, C. J. M., Chierici, M., David T, D., et al. (2023). Plankton dynamics in Kongsfjorden during two years of contrasting environmental conditions. *Prog. Oceanogr.* 213:102996. https://doi.org/10.1016/j.pocean.2023.102996

608 Bertrand P, Strøm H, Bêty J, Steen H and others (2021) Feeding at the front line: interannual
609 variation in the use of glacier fronts by foraging black-legged kittiwakes. Mar Ecol Prog Ser
610 677:197-208. https://doi.org/10.3354/meps13869
611 Błaszczyk, M., Jania, J., & Hagen, J. O. (2009). Tidewater glaciers of Svalbard: Recent changes
612 and estimates of calving fluxes.
613 Björkman, M.P., Zarsky, J.D., Kühnel, R., Hodson, A., Sattler, B. and Psenner, R., (2014).
614 Microbial cell retention in a melting High Arctic snowpack, Svalbard. *Arctic, antarctic, and*
615 *alpine research*, *46*(2), pp.471-482.
616 Cape, M.R., Straneo, F., Beaird, N. *et al.* (2019): Nutrient release to oceans from buoyancy-
617 driven upwelling at Greenland tidewater glaciers. *Nature Geosci* **12**, 34–39.
618 https://doi.org/10.1038/s41561-018-0268-4
619 Cottier, F., Tverberg, V., Inall, M., et al., (2005). Water mass modification in an Arctic fjord
620 through cross-shelf exchange: the seasonal hydrography of Kongsfjorden. Svalbard. J. Geophys.
621 Res. 110, C12005. https://doi.org/10.11029/12004JC002757.
622 Filhol, S., Lefeuvre, P. M., Ibañez, J. D., Hulth, J., Hudson, S. R., Gallet, J. C., ... & Burkhart, J.
623 F. (2023). A new approach to meteorological observations on remote polar glaciers using open-
624 source internet of things technologies. *Frontiers in Environmental Science*, *11*, 1085708.
625 https://doi.org/10.3389/fenvs.2023.1085708
626 Flowers, G. E. (2015). Modelling water flow under glaciers and ice sheets. *Proceedings of the*
627 *Royal Society A: Mathematical, Physical and Engineering Sciences*, *471*(2176), 20140907.
628 https://doi.org/10.1098/rspa.2014.0907
629 Geyman, E. C., JJ van Pelt, W., Maloof, A. C., Aas, H. F., & Kohler, J. (2022). Historical glacier
630 change on Svalbard predicts doubling of mass loss by 2100. *Nature*, *601*(7893), 374-379.
631 Grasshoff K (1965) On the Automatic Determination of Phosphate, Silicate and Fluoride in
632 Seawater. ICES Hydrographic Committee Report No. 129
633 Gundersen, K., Møgster, J.S., Lien, V.S. *et al.* (2022) Thirty Years of Nutrient Biogeochemistry
634 in the Barents Sea and the adjoining Arctic Ocean, 1990–2019. *Sci Data* **9**, 649.
635 https://doi.org/10.1038/s41597-022-01781-w
636 Hagen, J.O., O. Liestøl, E. Roland and T. Jørgensen. 1993. Glacier atlas of Svalbard and Jan
637 Mayen. Nor. Polarinst. Medd. 129.

638 Halbach, L., Vihtakari, M., Duarte, P., Everett, A., Granskog, M. A., Hop, H., ... & Assmy, P.
639 (2019). Tidewater glaciers and bedrock characteristics control the phytoplankton growth
640 environment in a fjord in the Arctic. *Frontiers in Marine Science*, *6*, 254.
641 https://doi.org/10.3389/fmars.2019.00254
642 Hodson, A., Porter, P., Lowe, A., & Mumford, P. (2002). Chemical denudation and silicate
643 weathering in Himalayan glacier basins: Batura Glacier, Pakistan. *Journal of Hydrology*, *262*(1-
644 4), 193-208. https://doi.org/10.1016/S0022-1694(02)00036-7
645 Hatton, J.E., Hendry, K.R., Hawkings, J.R., Wadham, J.L., Opfergelt, S., Kohler, T.J., Yde, J.C.,
646 Stibal, M. and Žárský, J.D., (2019): Silicon isotopes in Arctic and sub-Arctic glacial meltwaters:
647 the role of subglacial weathering in the silicon cycle. *Proceedings of the Royal Society A*,
648 *475*(2228), p.20190098.
649 Hodson, A., Mumford, P. and Lister, D., (2004): Suspended sediment and phosphorus in
650 proglacial rivers: bioavailability and potential impacts upon the P status of ice-marginal
651 receiving waters. *Hydrological processes*, *18*(13), pp.2409-2422.
652 Hodson, A.J., Mumford, P.N., Kohler, J. and Wynn, P.M., (2005). The High Arctic glacial
653 ecosystem: new insights from nutrient budgets. *Biogeochemistry*, *72*, pp.233-256.
654 Hodson, A., (2006a): Phosphorus in glacial meltwaters. *Glacier Science and Environmental*
655 *Change*, pp.81-82.
656 Hodson, A., (2006b): Biogeochemistry of snowmelt in an Antarctic glacial ecosystem. *Water*
657 *Resources Research*, *42*(11).
658 Hodson, A., Anesio, A.M., Tranter, M., Fountain, A., Osborn, M., Priscu, J., Laybourn-Parry, J.
659 and Sattler, B. (2008), GLACIAL ECOSYSTEMS. Ecological Monographs, 78: 41-67.
660 https://doi.org/10.1890/07-0187.1
661 Hop H, Wold A, Vihtakari M, Assmy P, Kuklinski P, Kwasniewski S, Griffith GP, Pavlova O,
662 Duarte P and Steen H (2023) Tidewater glaciers as “climate refugia” for zooplankton-dependent
663 food web in Kongsfjorden, Svalbard. Front. Mar. Sci. 10:1161912.
664 https://doi.org10.3389/fmars.2023.1161912
665 Hopwood, M.J., Carroll, D., Browning, T.J. *et al* (2018)*:* Non-linear response of summertime
666 marine productivity to increased meltwater discharge around Greenland. *Nat Commun* **9**, 3256.
667 https://doi.org/10.1038/s41467-018-05488-8

Hopwood, M. J., Carroll, D., Dunse, T., Hodson, A., Holding, J. M., Iriarte, J. L., Ribeiro, S., Achterberg, E. P., Cantoni, C., Carlson, D. F., Chierici, M., Clarke, J. S., Cozzi, S., Fransson, A., Juul-Pedersen, T., Winding, M. H. S., and Meire, L. (2020): Review article: How does glacier discharge affect marine biogeochemistry and primary production in the Arctic?, The Cryosphere, 14, 1347–1383, https://doi.org/10.5194/tc-14-1347-2020

How, P., Benn, D.I., Hulton, N.R., Hubbard, B., Luckman, A., Sevestre, H., Van Pelt, W.J., Lindbäck, K., Kohler, J. and Boot, W., (2017). Rapidly changing subglacial hydrological pathways at a tidewater glacier revealed through simultaneous observations of water pressure, supraglacial lakes, meltwater plumes and surface velocities. *The Cryosphere*, *11*(6), pp.2691-2710.

IPCC, (2019): IPCC Special Report on the Ocean and Cryosphere in a Changing Climate [H.-O. Pörtner, D.C. Roberts, V. Masson-Delmotte, P. Zhai, M. Tignor, E. Poloczanska, K. Mintenbeck, A. Alegría, M. Nicolai, A. Okem, J. Petzold, B. Rama, N.M. Weyer (eds.)]. Cambridge University Press, Cambridge, UK and New York, NY, USA, 755 pp. https://doi.org/10.1017/9781009157964

Isaksen, K., Nordli, Ø., Ivanov, B. *et al.* Exceptional warming over the Barents area. *Sci Rep* **12**, 9371 (2022). https://doi.org/10.1038/s41598-022-13568-5

James, M.R., Robson, S., d'Oleire-Oltmanns, S. and Niethammer, U., (2017). Optimising UAV topographic surveys processed with structure-from-motion: Ground control quality, quantity and bundle adjustment. *Geomorphology*, *280*, pp.51-66.

Juul-Pedersen, T., Arendt, K. E., Mortensen, J., Blicher, M. E., Søgaard, D. H., & Rysgaard, S. (2015). Seasonal and interannual phytoplankton production in a sub-Arctic tidewater outlet glacier fjord, SW Greenland. *Marine Ecology Progress Series*, *524*, 27-38. **https://doi.org/10.3354/meps11174**

Kanna, N., Sugiyama, S., Ohashi, Y., Sakakibara, D., Fukamachi, Y., & Nomura, D. (2018). Upwelling of macronutrients and dissolved inorganic carbon by a subglacial freshwater driven plume in Bowdoin Fjord, northwestern Greenland. *Journal of Geophysical Research: Biogeosciences*, 123, 1666–1682. https://doi.org/10.1029/2017JG004248

Kavan, J., Luláková, P., Małecki, J., & Strzelecki, M. (2023). Capturing the transition from marine to land-terminating glacier from the 126-year retreat history of Nordenskiöldbreen, Svalbard. *Journal of Glaciology*, 1-11. doi:10.1017/jog.2023.92

699 Kjeldsen, K. K., Mortensen, J., Bendtsen, J., Petersen, D., Lennert, K., and Rysgaard, S. (2014),
700 Ice-dammed lake drainage cools and raises surface salinities in a tidewater outlet glacier fjord,
701 west Greenland, *J. Geophys. Res. Earth Surf.*, 119, 1310–1321,
702 https://doi.org/10.1002/2013JF003034.
703 Kohler, J., James, T. D., Murray, T., Nuth, C., Brandt, O., Barrand, N. E., Aas, H. F., and
704 Luckman, A. (2007), Acceleration in thinning rate on western Svalbard glaciers, *Geophys. Res.*
705 *Lett.*, 34, L18502, doi:10.1029/2007GL030681.
706 Konik, M., Darecki, M., Pavlov, A. K., Sagan, S., & Kowalczuk, P. (2021). Darkening of the
707 Svalbard Fjords waters observed with satellite ocean color imagery in 1997–2019. *Frontiers in*
708 *Marine Science*, *8*, 699318. https://doi.org/10.3389/fmars.2021.699318
709 Lea, J. M. (2018): The Google Earth Engine Digitisation Tool (GEEDiT) and the Margin change
710 Quantification Tool (MaQiT) – simple tools for the rapid mapping and quantification of
711 changing Earth surface margins, Earth Surf. Dynam., 6, 551–561, https://doi.org/10.5194/esurf-
712 6-551-2018
713 LiestøL O, 1976. Setevatnet, a glacier dammed lake in Spitsbergen. Norsk Polarinstitutt Årbok
714 1975, 31-35.
715 Lydersen, C., Assmy, P., Falk-Petersen, S., Kohler, J., Kovacs, K. M., Reigstad, M., ... &
716 Zajaczkowski, M. (2014). The importance of tidewater glaciers for marine mammals and
717 seabirds in Svalbard, Norway. *Journal of Marine Systems*, *129*, 452-471.
718 https://doi.org/10.1016/j.jmarsys.2013.09.006
719 McDougall, T.J. and P.M. Barker, (2011): Getting started with TEOS-10 and the Gibbs Seawater
720 (GSW) Oceanographic Toolbox, 28pp., SCOR/IAPSO WG127, ISBN 978-0-646-55621-5.
721 Meire, L., Mortensen, J., Meire, P., Juul-Pedersen, T., Sejr, M. K., Rysgaard, S., ... & Meysman,
722 F. J. (2017). Marine-terminating glaciers sustain high productivity in Greenland fjords. *Global*
723 *Change Biology*, *23*(12), 5344-5357. https://doi.org/10.1111/gcb.13801
724 Melvold K, Ove Hagen J. Evolution of a Surge-Type Glacier in its Quiescent Phase:
725 Kongsvegen, Spitsbergen, 1964–95. *Journal of Glaciology*. 1998;44(147):394-404.
726 doi:10.3189/S0022143000002720
727 NPI, 2023. *Norwegian Polar Institute, University of Oslo (2023). Cumulative mass balance for*
728 *glaciers in Svalbard. Environmental monitoring of Svalbard and Jan Mayen (MOSJ). URL:*
729 *http://www.mosj.no/en/climate/land/mass-balance-glaciers.html*

Pavlov, A. K., Leu, E., Hanelt, D., Bartsch, I., Karsten, U., Hudson, S. R., ... & Granskog, M. A. (2019). The underwater light climate in Kongsfjorden and its ecological implications. *The Ecosystem of Kongsfjorden, Svalbard*, 137-170.

Rantanen, M., Karpechko, A. Y., Lipponen, A., Nordling, K., Hyvärinen, O., Ruosteenoja, K., Vihma, T., and Laaksonen, A., (2022): The Arctic has warmed nearly four times faster than the globe since 1979, Communications Earth & Environment, 3, 168, https://doi.org/10.1038/s43247-022-00498-3

Roberts, T.J., Hodson, A., Evans, C.D. and Holmén, K. (2010): Modelling the impacts of a nitrogen pollution event on the biogeochemistry of an Arctic glacier. *Annals of Glaciology*, *51*(56), pp.163-170.

Schiøtt, S., Tejsner, P. & Rysgaard, S. (2022): Inuit and Local Knowledge on the Marine Ecosystem in Ilulissat Icefjord, Greenland. *Hum Ecol* **50**, 167–181. https://doi.org/10.1007/s10745-021-00277-2

Schmidt, L. S., Schuler, T. V., Thomas, E. E. (2023), and Westermann, S.: Meltwater runoff and glacier mass balance in the high Arctic: 1991–2022 simulations for Svalbard, The Cryosphere, 17, 2941–2963, https://doi.org/10.5194/tc-17-2941-2023

Schuler, T.V., Kohler, J., Elagina, N., Hagen, J.O.M., Hodson, A.J., Jania, J.A., Kääb, A.M., Luks, B., Malecki, J., Moholdt, G., Pohjola, V.A., Sobota, I., Van Pelt, W.J.J. (2020). Reconciling Svalbard glacier mass balance. *Front. Earth Sci*., doi: 10.3389/feart.2020.00156

Shugar, D.H., Burr, A., Haritashya, U.K. *et al.* Rapid worldwide growth of glacial lakes since 1990. *Nat. Clim. Chang.* **10**, 939–945 (2020). https://doi.org/10.1038/s41558-020-0855-4

Spolaor, A., Varin, C., Pedeli, X., Christille, J.M., Kirchgeorg, T., Giardi, F., Cappelletti, D., Turetta, C., Cairns, W.R., Gambaro, A. and Bernagozzi, A., (2021): Source, timing and dynamics of ionic species mobility in the Svalbard annual snowpack. *Science of the Total Environment*, *751*, p.141640.

Stott, F. C. (1936). The Marine Foods of Birds in an Inland Fjord Region in West Spitsbergen: Part 1. Plankton and in Shore Benthos. *Journal of Animal Ecology*, *5*(2), 356–369. https://doi.org/10.2307/1040

Tallentire, G.D., Shiggins, C.J., Rawlins, L.D., Evans, J. and Hodgkins, R., 2023. Observing relationships between sediment-laden meltwater plumes, glacial runoff and a retreating terminus at Blomstrandbreen, Svalbard. *International Journal of Remote Sensing*, *44*(13), pp.3972-3992.

761 Torsvik, T., Albretsen, J., Sundfjord, A., Kohler, J., Sandvik, A. D., Skarðhamar, J., ... & Everett,
762 A. (2019). Impact of tidewater glacier retreat on the fjord system: Modeling present and future
763 circulation in Kongsfjorden, Svalbard. *Estuarine, Coastal and Shelf Science*, *220*, 152-165.
764 https://doi.org/10.1016/j.ecss.2019.02.005
765 Tranter, M., Skidmore, M. and Wadham, J., (2005). Hydrological controls on microbial
766 communities in subglacial environments. *Hydrological Processes*, *19*(4), pp.995-998.
767 van Pelt, W., Pohjola, V., Pettersson, R., Marchenko, S., Kohler, J., Luks, B., Hagen, J. O.,
768 Schuler, T. V., Dunse, T., Noël, B., and Reijmer, C. (2019): A long-term dataset of climatic mass
769 balance, snow conditions, and runoff in Svalbard (1957–2018), The Cryosphere, 13, 2259–2280,
770 https://doi.org/10.5194/tc-13-2259-2019
771 Valiente, N., Eiler, A., Allesson, L., Andersen, T., Clayer, F., Crapart, C., Dörsch, P., Fontaine,
772 L., Heuschele, J., Vogt, R.D., Wei, J., de Wit, H.A., and Hessen, D.O. (2022) Catchment
773 properties as predictors of greenhouse gas concentrations across a gradient of boreal lakes.
774 *Front. Environ. Sci.* **10**:880619. https://doi.org/10.3389/fenvs.2022.880619
775 Vionnet, V., Brun, E., Morin, S., Boone, A., Faroux, S., Le Moigne, P., Martin, E., and
776 Willemet, J.-M.(2012): The detailed snowpack scheme Crocus and its implementation in
777 SURFEX v7.2, Geosci. Model Dev., 5, 773–791, https://doi.org/10.5194/gmd-5-773-2012
778 Wadham, J.L., Tranter, M., Hodson, A.J., Hodgkins, R., Bottrell, S., Cooper, R. and Raiswell,
779 R., (2010). Hydro-biogeochemical coupling beneath a large polythermal Arctic glacier:
780 Implications for subice sheet biogeochemistry. *Journal of Geophysical Research: Earth Surface*,
781 *115*(F4).
782 Wei, J., Fontaine, L., Valiente, N. *et al.* (2023): Trajectories of freshwater microbial genomics
783 and greenhouse gas saturation upon glacial retreat. *Nat Commun* **14**, 3234.
784 https://doi.org/10.1038/s41467-023-38806-w
785 Westermann, S., Ingeman-Nielsen, T., Scheer, J., Aalstad, K., Aga, J., Chaudhary, N.,
786 Etzelmüller, B., Filhol, S., Kääb, A., Renette, C., Schmidt, L. S., Schuler, T. V., Zweigel, R. B.,
787 Martin, L., Morard, S., Ben-Asher, M., Angelopoulos, M., Boike, J., Groenke, B., Miesner, F.,
788 Nitzbon, J., Overduin, P., Stuenzi, S. M., and Langer, M. (2023): The CryoGrid community
789 model (version 1.0) – a multi-physics toolbox for climate-driven simulations in the terrestrial
790 cryosphere, Geosci. Model Dev., 16, 2607–2647, https://doi.org/10.5194/gmd-16-2607-2023

Williams, P. L., Burgess, D. O., Waterman, S., Roberts, M., Bertrand, E. M., & Bhatia, M. P. (2021). Nutrient and carbon export from a tidewater glacier to the coastal ocean in the Canadian Arctic Archipelago. *Journal of Geophysical Research: Biogeosciences*, 126, e2021JG006289. https://doi.org/10.1029/2021JG006289

Wynn, P.M., Hodson, A. and Heaton, T., 2006. Chemical and isotopic switching within the subglacial environment of a High Arctic glacier. *Biogeochemistry*, *78*, pp.173-193.

Zakem, E.J., Al-Haj, A., Church, M.J. *et al.* Ecological control of nitrite in the upper ocean. *Nat Commun* **9**, 1206 (2018). https://doi.org/10.1038/s41467-018-03553-w